Transactions on Additive Manufacturing Meets Medicine
Trans. AMMM, 2025, Vol. 7, No 1, Article ID 2062, 4 Pages

Infinite Science Publishing

Original Research Article

Guided Bone Regeneration: A novel approach to 3D-printed biodegradable meshes

T. Strunk[1,2,3*], F.M. Thieringer[1,2], N. Rohr[3†], and N. Sharma[1,2†]

[1] *Medical Additive Manufacturing Research Group (Swiss MAM), Department of Biomedical Engineering, University of Basel, Allschwil, Switzerland*
[2] *Clinic of Oral and Cranio-Maxillofacial Surgery, University Hospital Basel, Basel, Switzerland*
[3] *Biomaterials and Technology, Department Research, University Center for Dental Medicine Basel UZB, University of Basel, Basel, Switzerland*
[*] *Corresponding author, email: till.strunk@unibas.ch.*
†These authors have contributed equally and share the last authorship.

Abstract: Guided Bone Regeneration (GBR) is a standard surgical procedure to augment jawbone volume, conventionally using titanium meshes or collagen membranes - each with inherent limitations such as stress shielding, imaging artifacts, or insufficient mechanical stability. Here, we introduce a novel 3D-printed, patient-specific biodegradable mesh fabricated via Arburg plastic freeforming (APF) using PLDLLA/β-TCP composite. Three design variants were fabricated: A solid configuration for maximal strength and porous or gyroid structures (50% infill) to promote cell integration. Our results demonstrate high dimensional accuracy (<1% deviation) and pore sizes of 243±17 µm (porous) and 620±64 µm (gyroid). Mechanical testing revealed that the solid design achieved a biaxial flexural strength of 129±13 MPa, significantly outperforming the porous (26±5 MPa) and gyroid designs (23±2 MPa). Surface roughness (Ra) characterization yielded significantly higher values for porous (2.27±0.38 µm) and gyroid (1.3±0.2 µm) samples, potentially improving protein adhesion and osseointegration. These results lay the foundation for further optimization, including hybrid designs that integrate robust mechanical support with favorable biological properties, ultimately eliminating the need for secondary surgery.

I. Introduction

Oral- and Maxillofacial Surgery (OMFS) often necessitates bone augmentation before procedures like dental implantations. Traditional Guided Bone Regeneration (GBR) meshes – whether metallic (e.g. titanium) or biodegradable (e.g. collagen) – present challenges [1]. Titanium is mechanically robust but may induce stress shielding and require removal surgery, whereas collagen lacks sufficient stability for some augmentations [1,2]. We propose a three-dimensionally (3D)-printed, patient-specific biodegradable mesh produced using Arburg plastic freeforming (APF) technology to overcome these limitations. Utilizing a medical grade Poly(L-lactide-co-D,L-lactide) (PLDLLA) and β-tricalcium phosphate (β-TCP) composite, our approach combines adequate mechanical integrity with controlled biodegradation, reducing patient morbidity and healthcare costs by eliminating a second surgical intervention.

Using β-TCP alongside a biodegradable polymer may increase the osteogenic ability and degradation rate of the composite, making it more suitable for matching tissue regeneration needs [3,4].

Triply periodic minimal surface patters like gyroid have been shown to improve cell proliferation [5]. Applying them to a GBR mesh could lead to an enhanced surgery outcome by improving the bone regeneration into the implant.

This study aims to investigate APF printing parameters that enable dimensionally accurate 3D printing of designs and subsequent suitability for later application as a mesh in GBR.

Infinite Science Publishing

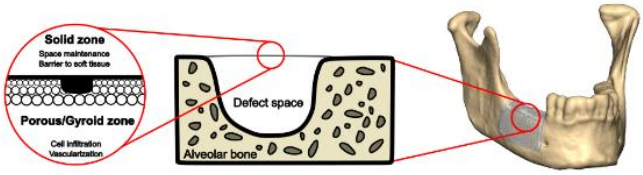

Figure 1: Schematic image of a GBR mesh. Applying different designs into a hybrid mesh could combine advantages of each design.

II. Materials and methods

A medical grade composite material made of PLDLLA and β-TCP (Resomer Composite LR 706 S β-TCP, Evonik, Essen, Germany) was used to fabricate specimens using APF (Freeformer 300-3X, Arburg, Lossburg, Germany). Three design types were developed: Solid disks with a diameter of 12 mm and height of 1 mm were created as standard tessellation language (STL) files with Inventor 2024 (Autodesk, San Rafael, USA). Porous samples were derived from the solid design by applying a 50% infill using the Arburg slicer. Given the fixed nozzle diameter, this value was expected to result in a osteoconductivity-promoting pore size. Gyroid samples with the same porosity were generated using a gyroid function in nTop (nTopology, New York, USA) with an added 0.4 mm rim to enhance edge stability. Key parameters (e.g., nozzle temperatures, print bed temperature, droplet aspect ratio and discharge rate) were optimized to achieve high dimensional accuracy (<1% deviation in both XY and Z directions) and the desired pore architecture. To assess this, cubes (n=3) with 15 mm edge length were 3D-printed using the same three designs and subsequently imaged with light microscopy and measured using a caliper (WZ0031, Logilink GmbH, Germany; resolution: 10 µm). Detailed parameters are summarized in Table 1.

Table 1: Arburg plastic freeforming printing parameters.

Design	Solid	Porous	Gyroid
Print temperatures (T_{nozzle},T_2,T_1,T_{input}) [°C]	190, 185, 170, 45	190, 185, 170, 45	190, 185, 170, 45
Print bed temperature [°C]	50	50	50
Layer height [µm]	200	200	200
Droplet aspect ratio (DAR)	1.32	1.25	1.27
Discharge rate (DR)	69 %	70 %	54 %

For subsequent material characterizations, the disk-shaped specimens were used (n=15). The surface wettability with water was assessed using the sessile droplet method and a drop shape analyzer (DSA30, Krüss, Hamburg, Germany). The arithmetical mean height surface roughness parameter (Ra) was acquired using a confocal laser scanning microscope (Keyence VK-X1050, Osaka, Japan). The specimens' biaxial flexural strength was obtained at a 1 mm/min cross-head speed with a universal testing machine (Zwick/Roell, Ulm, Germany).

III. Results and discussion

Dimensional accuracy and pore characteristics

The 3D-printed samples exhibited excellent fidelity, with deviations of less than 1% (Table 2 and Fig. 2). Porous designs showed pore sizes averaging 243±17 µm - ideal for reducing fibrous tissue ingrowth - while the gyroid design yielded significantly larger pores (620±64 µm, $p<0.0001$), which may promote angiogenesis [6,7].

Although earlier studies favored 300-500 µm pores, recent evidence supports larger pore sizes (up to 1200 µm) for vascularization or around 600 µm in mandibular applications [7-9].

Table 2: Dimensional accuracy of 3D printed cubes with a 15 mm edge length, measured with a caliper in XY (width) or Z direction (height). The pore size was calculated using light microscopy images from atop and appropriate software. N = 3.

Sample Design	Solid	Porous	Gyroid
Dimensional Accuracy XY	0.84%	-0.33%	0.23%
Dimensional Accuracy Z	0.20%	0.54%	0.18%
Pore Size [µm]		243±17	620±64

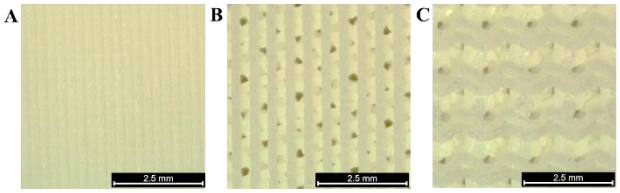

Figure 2: Morphologies of solid (A), porous (B) and gyroid (C) specimens imaged with light microscopy.

Surface properties

Surface roughness parameter Ra of porous samples was 2.27±0.38 µm (Fig. 3A), potentially favoring protein adsorption and subsequent cell adhesion [10]. Osteoblast integration on titanium surfaces has been shown to be optimal between 1-2 µm, suggesting that gyroid samples (1.3±0.2 µm) present an ideal roughness for osseointegration [11].

Interestingly, the solid design demonstrated lower Ra values - possibly due to a slower cooling rate allowing improved droplet fusion. This effect merits further investigation and may have caused the lower contact angle for solid samples (92°, Fig. 3B). More hydrophilic surfaces (contact angle ≤ 80°) are reported to improve further cell adhesion on a synthetic polymer [12].

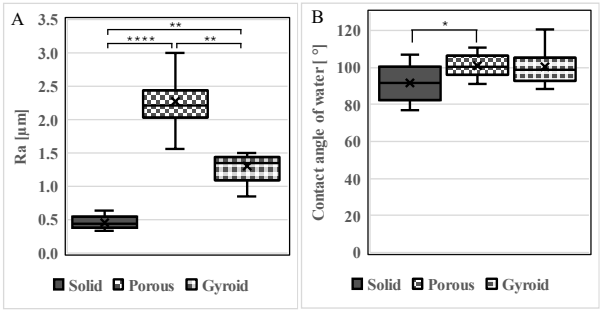

*Figure 3: A) Surface roughness parameter Ra obtained on top of a sample's strand. B) The contact angle of water is different for each design. Statistical differences using Kruskal-Wallis and subsequent Dunn's test are indicated with *(p<0.05), ** (p<0.01) or **** (p<0.0001). Each box indicates the sample's interquartile range and median. The mean is indicated by an X. N=15.*

Mechanical Performance

Biaxial flexural testing showed that the solid configuration achieved a strength of 129±13 MPa, significantly higher than the porous (26±5 MPa) and gyroid (23±2 MPa) designs (Fig. 4). Under physiological conditions, loads of circa 30 N can be expected, leading to a simulated maximum stress of 9.9 MPa in solid Polycaprolactone scaffolds [13].

While titanium meshes are expected to endure higher bending strengths in the range of 267-512 MPa, and PEEK meshes yield 20-30 MPa, our biodegradable composite offers a competitive balance between mechanical strength and bioresorbability [14,15].

The observed trade-off between mechanical strength and pore-mediated biological potential suggests that a hybrid design - integrating solid beams with targeted porous regions - could optimize load-bearing capacity for low-load applications and tissue integration.

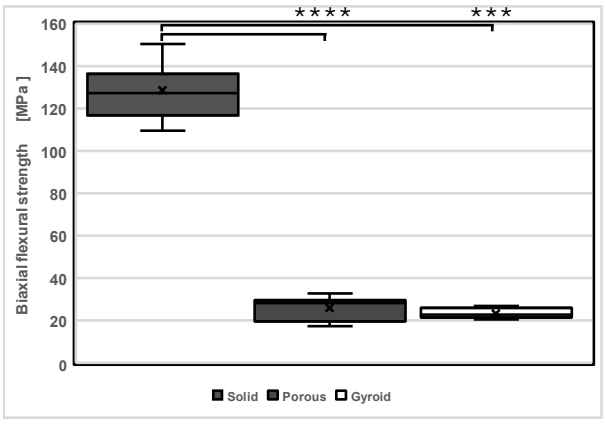

*Figure 4: Biaxial flexural strength displayed in MPa was obtained at a cross-head speed of 1 mm/min. Each box indicates the sample's interquartile range and median. The mean is marked by an X. Statistical differences using Kruskal-Wallis and subsequent Dunn's test are indicated with ***(p<0.001) or ****(p<0.0001). N =15.*

IV. Conclusions

This study presents a promising proof-of-concept for APF-3D-printed, patient-specific biodegradable meshes in GBR applications. The solid design provides exceptional mechanical strength, while the porous and gyroid structures offer pore architectures conducive to tissue integration. Future research will focus on developing hybrid designs, assessing the impact of sterilization techniques, and conducting in vitro/in vivo evaluations to determine cellular responses and degradation behavior. The results of this study were obtained in vitro and may not reliably reflect in vivo behavior, as the complex environment may significantly alter the material's performance. Ultimately, our approach aims to improve GBR outcomes by merging mechanical and biological advantages while eliminating the need for secondary surgical procedures.

Acknowledgments

The authors thank Sabrina Karlin for the technical support during mechanical testing, contact angle and surface roughness measurements. We thank the Osteology foundation for the financial support (Project No: 22-126). Furthermore, this work was funded by the Innovation Focus - Regenerative Surgery of the University Hospital Basel and by the Werner Siemens Foundation through the Minimally Invasive Robot-Assisted Computer-guided LaserosteotomE II (MIRACLEII) project.

Author's Statement

Authors state no conflict of interest. No animal experiments were carried out. Consent was obtained from all persons involved in this study. The research related to human use complies with all the relevant national regulations, institutional policies and was performed in accordance with the tenets of the Helsinki Declaration, and has been approved by the authors' institutional review board or equivalent committee.

References

[1] K. Kim, Y. Su, A. J. Kucine, K. Cheng, and D. Zhu, "Guided bone regeneration using barrier membrane in dental applications," *ACS Biomaterials Science & Engineering*, vol. 9, no. 10, pp. 5457-5478, 2023.

[2] K. Yaqoob, I. Amjad, M. A. Munir Awan, U. Liaqat, M. Zahoor, and M. Kashif, "Novel method for the production of titanium foams to reduce stress shielding in implants," *ACS Omega*, vol. 8, no. 2, pp. 1876-1884, 2023

[3] L. Cao, P.-G. Duan, H.-R. Wang, X.-L. Li, F.-L. Yuan, Z.-Y. Fan, S.-M. Li, and J. Dong, "Degradation and osteogenic potential of a novel poly (lactic acid)/nano-sized β-tricalcium phosphate scaffold," *International Journal of Nanomedicine*, pp. 5881–5888, 2012.

[4] W. Wang, P. Liu, B. Zhang, X. Gui, X. Pei, P. Song, X. Yu, Z. Zhang, and C. Zhou, "Fused deposition modeling printed PLA/Nano β-TCP composite bone tissue engineering scaffolds for promoting osteogenic induction function," *International Journal of Nanomedicine*, pp. 5815–5830, 2023.

[5] W. Guo, Y. Yang, C. Liu, W. Bu, F. Guo, J. Li, E. Wang, Z. Peng, H. Mai, and H. You, "3D printed TPMS structural PLA/GO scaffold: Process parameter optimization, porous structure, mechanical and biological properties," *Journal of the Mechanical Behavior of Biomedical Materials*, vol. 142, p. 105848, 2023.

[6] K. Hayashi, M. Shimabukuro, R. Kishida, A. Tsuchiya, and K. Ishikawa, "Honeycomb scaffolds capable of achieving barrier membrane-free guided bone regeneration," *Materials Advances*, vol. 2, no. 23, pp. 7638–7649, 2021.

[7] C. Ghayor and F. E. Weber, "Osteoconductive microarchitecture of bone substitutes for bone regeneration revisited," *Frontiers in Physiology*, vol. 9, p. 960, 2018.

[8] G. Turco, E. Marsich, F. Bellomo, S. Semeraro, I. Donati, F. Brun, M. Grandolfo, A. Accardo, and S. Paoletti, "Alginate/hydroxyapatite biocomposite for bone ingrowth: a trabecular structure with high and isotropic connectivity," *Biomacromolecules*, vol. 10, no. 6, pp. 1575–1583, 2009.

[9] H. Qin, Y. Wei, J. Han, X. Jiang, X. Yang, Y. Wu, Z. Gou, and L. Chen, "3D printed bioceramic scaffolds: adjusting pore dimension is beneficial for mandibular bone defects repair," *Journal of Tissue Engineering and Regenerative Medicine*, vol. 16, no. 4, pp. 409–421, 2022.

[10] F. Chen, C. N. Lee, and S. H. Teoh, "Nanofibrous modification on ultra-thin poly (e-caprolactone) membrane via electrospinning," *Materials Science and Engineering: C*, vol. 27, no. 2, pp. 325-332, 2007.

[11] O. Andrukhov, R. Huber, B. Shi, S. Berner, X. Rausch-Fan, A. Moritz, N. D. Spencer, and A. Schedle, "Proliferation, behavior, and differentiation of osteoblasts on surfaces of different microroughness," *Dental Materials*, vol. 32, no. 11, pp. 1374–1384, 2016.

[12] J. Wei, T. Igarashi, N. Okumori, T. Igarashi, T. Maetani, B. Liu, and M. Yoshinari, "Influence of surface wettability on competitive protein adsorption and initial attachment of osteoblasts," *Biomedical Materials*, vol. 4, no. 4, p. 045002, 2009.

[13] P. Vilanova-Corrales, E. Demiquels-Punzano, J. Caballé-Serrano, F. Hernández-Alfaro, J. Á. Delgado, R. A. Pérez, J. Gil, and L. M. Delgado, "Biodegradable and reinforced membranes based on polycaprolactone and collagen for guided bone regeneration," *Materials Today Communications*, vol. 41, p. 111039, 2024.

[14] X.-R. Zhu, C. Chen, Y.-W. Hua, X.-Y. Xu, P. Song, R.-Y. Wang, and C.-X. Wang, "A comparative quantitative assessment of 3D-printed PEKK and PEEK thin meshes in customized alveolar bone augmentation," *BMC Oral Health*, vol. 24, no. 1, p. 1304, 2024.

[15] L. Bai, P. Ji, X. Li, H. Gao, L. Li, and C. Wang, "Mechanical characterization of 3D-printed individualized Ti-mesh (membrane) for alveolar bone defects," *Journal of Healthcare Engineering*, vol. 2019, no. 1, p. 4231872, 2019.